

## FIRST experiment: Fragmentation of Ions Relevant for Space and Therapy

This content has been downloaded from IOPscience. Please scroll down to see the full text.

2013 J. Phys.: Conf. Ser. 420 012061

(<http://iopscience.iop.org/1742-6596/420/1/012061>)

View [the table of contents for this issue](#), or go to the [journal homepage](#) for more

Download details:

IP Address: 192.84.151.58

This content was downloaded on 28/10/2015 at 16:57

Please note that [terms and conditions apply](#).

## FIRST experiment: Fragmentation of Ions Relevant for Space and Therapy

C Agodi<sup>6</sup>, Z Abou-Haidar<sup>16</sup>, M A G Alvarez<sup>16</sup>, T Aumann<sup>1</sup>, F Balestra<sup>8</sup>, G Battistoni<sup>2</sup>, A Bocci<sup>16</sup>, T T Bohlen<sup>22,23</sup>, M Bondi<sup>6,27</sup>, A Boudard<sup>21</sup>, A Brunetti<sup>3,9</sup>, M Carpinelli<sup>3,13</sup>, F Cappuzzello<sup>27,6</sup>, M Cavallaro<sup>6</sup>, D Carbone<sup>6,27</sup>, G A P Cirrone<sup>6</sup>, M A Cortes-Giraldo<sup>17</sup>, G Cuttone<sup>6</sup>, M De Napoli<sup>4</sup>, M Durante<sup>1</sup>, J P Fernandez-Garcia<sup>17</sup>, C Finck<sup>1</sup>, A Foti<sup>4,27</sup>, M I Gallardo<sup>17</sup>, B Golosio<sup>3,13</sup>, E Iarocci<sup>5,10</sup>, F Iazzi<sup>8,11</sup>, G. Ickert<sup>1</sup>, R Introzzi<sup>8</sup>, D Juliani<sup>18</sup>, J Krimmer<sup>20</sup>, N Kurz<sup>1</sup>, M Labalme<sup>8</sup>, A Lavagno<sup>8,11</sup>, Y Leifels<sup>1</sup>, A Le Fevre<sup>1</sup>, S Leray<sup>21</sup>, F Marchetto<sup>8</sup>, V Monaco<sup>8,12</sup>, M C Morone<sup>9,14</sup>, D Nicolosi<sup>27,6</sup>, P Oliva<sup>3,13</sup>, A Paoloni<sup>5</sup>, V Patera<sup>5,10</sup>, L Piersanti<sup>5,10</sup>, R Pleskac<sup>1</sup>, J M Quesada<sup>17</sup>, N Randazzo<sup>4</sup>, F Romano<sup>6,15</sup>, D Rossi<sup>1</sup>, V Rosso<sup>25,26</sup>, M Rousseau<sup>18</sup>, R Sacchi<sup>8,12</sup>, P Sala<sup>2</sup>, A Sarti<sup>5,10</sup>, C Scheidenberger<sup>1</sup>, C Schuy<sup>1</sup>, A Sciubba<sup>5,10</sup>, C Sffienti<sup>24</sup>, H Simon<sup>1</sup>, V Sipala<sup>3,13</sup>, E Spiriti<sup>7</sup>, L Stuttge<sup>18</sup>, S Tropea<sup>6,27</sup> and H Younis<sup>8,11</sup>

<sup>1</sup>GSI Helmholtzzentrum für Schwerionenforschung, Darmstadt, Germany

<sup>2</sup>Istituto Nazionale di Fisica Nucleare - Sezione di Milano, Italy

<sup>3</sup>Istituto Nazionale di Fisica Nucleare - Sezione di Cagliari, Italy

<sup>4</sup>Istituto Nazionale di Fisica Nucleare - Sezione di Catania, Italy

<sup>5</sup>Istituto Nazionale di Fisica Nucleare - Laboratori Nazionali di Frascati, Italy

<sup>6</sup>Istituto Nazionale di Fisica Nucleare - Laboratori Nazionali del Sud, Catania - Italy

<sup>7</sup>Istituto Nazionale di Fisica Nucleare - Sezione di Roma 3, Italy

<sup>8</sup>Istituto Nazionale di Fisica Nucleare - Sezione di Torino, Italy

<sup>9</sup>Istituto Nazionale di Fisica Nucleare - Sezione di Roma Tor Vergata, Italy

<sup>10</sup>Dipartimento di Scienze di Base e Applicate per l'Ingegneria, "La Sapienza"

Università di Roma, Italy

<sup>11</sup>Dipartimento di Fisica, Politecnico di Torino, Italy

<sup>12</sup>Dipartimento di Fisica, Università di Torino, Italy

<sup>13</sup>Università di Sassari, Italy

<sup>14</sup>Dipartimento di Biopatologia e Diagnostica per Immagini, Università di Roma Tor Vergata, Italy

<sup>15</sup>Centro Studi e Ricerche e Museo Storico della Fisica "Enrico Fermi", Roma, Italy

<sup>16</sup>CNA, Sevilla, Spain

<sup>17</sup>Departamento de Física Atomica, Molecular y Nuclear, University of Sevilla, 41080-Sevilla, Spain

<sup>18</sup>Institut Pluridisciplinaire Hubert Curien, Strasbourg, France

<sup>19</sup>LPC-Caen, ENSICAEN, Université de Caen, CNRS/IN2P3, Caen, France

<sup>20</sup>IPN-Lyon, Université de Lyon, Université Lyon 1, CNRS/IN2P3, Villeurbanne, France

<sup>21</sup>CEA-Saclay, IRFU/SPhN, Gif sur Yvette Cedex, France

<sup>22</sup>European Organization for Nuclear Research CERN, Geneva, Switzerland

<sup>23</sup>Medical Radiation Physics, Karolinska Institutet and Stockholm University, Stockholm, Sweden

<sup>24</sup>Universitat Mainz Johann-Joachim-Becher, Mainz, Germany

<sup>25</sup>Dipartimento di Fisica, Università di Pisa, Italy

<sup>26</sup>Istituto Nazionale di Fisica Nucleare - Sezione di Pisa, Italy

<sup>27</sup>Dipartimento di Fisica, Università di Catania, Italy

E-mail: agodi@lns.infn.it

**Abstract.** Nuclear fragmentation processes are relevant in different fields of basic research and applied physics and are of particular interest for tumor therapy and for space radiation protection applications. The FIRST (Fragmentation of Ions Relevant for Space and Therapy) experiment at SIS accelerator of GSI laboratory in Darmstadt, has been designed for the measurement of different ions fragmentation cross sections at different energies between 100 and 1000 MeV/nucleon. The experiment is performed by an international collaboration made of institutions from Germany, France, Italy and Spain. The experimental apparatus is partly based on an already existing setup made of the ALADIN magnet, the MUSIC IV TPC, the LAND2 neutron detector and the TOFWALL scintillator TOF system, integrated with newly designed detectors in the interaction Region (IR) around the carbon removable target: a scintillator Start Counter, a Beam Monitor drift chamber, a silicon Vertex Detector and a Proton Tagger for detection of light fragments emitted at large angles (KENTROS). The scientific program of the FIRST experiment started on summer 2011 with the study of the 400 MeV/nucleon  $^{12}\text{C}$  beam fragmentation on thin (8mm) carbon target.

## 1. Introduction

The driving force of radiotherapy is the search for higher precision and greater biological effectiveness of the applied dose and the transition from radiation to light particles for clinical beams goes in this direction.

In radiation treatments light ions presents some advantages, respect to standard radiations, essentially due to a better spatial selectivity in dose deposition (Bragg Peak), to a reduced lateral and longitudinal diffusion, to an high conformal dose deposition and to an high Biological effectiveness [1]. All these motivations made hadrontherapy a very good way to treat highly radiation resistant tumors, sparing surrounding organ at risk (OAR). Among ions, carbon presents a lot of advantages. For example, respect to protons, carbon ions have a more precise energy depositions, due to a lower lateral and longitudinal diffusion, and they have an optimal relative biological effectiveness (RBE) as a function of the penetration depth profile. Among other advantages, carbon ions allows the online PET, for depth deposition monitoring, and present a good compromise between RBE and Oxygen enhancement ratio (OER).

On the other hand, there are also some disadvantages in the use of carbon ions for therapy. The most relevant is due to nuclear fragmentation in the interaction processes with energy degraders and biological tissues [2]. Moreover, in these processes there is a production of fragments with velocities similar to the beam, but with higher range and a different biological effectiveness respect to the primary ions. For these reasons fragmentation determine a mitigation and an attenuation of the primary beam. Simulations with analytical codes are used to estimate how projectile fragmentation modifies dose distribution and biological effectiveness [3,4]. Such approach presents considerable uncertainty in the models implemented because of a reduced number of experimental data, both on the fragmentation cross sections and on the different quality of radiations biological effectiveness. Currently the treatment planning systems are generally based on deterministic codes, which are relatively fast. However in order to reach the accuracy required for medical applications (few% or less) the deterministic calculations must be refined and compared with Monte Carlo simulations [5]. Moreover, nuclear models, implemented both in FLUKA and GEANT4 codes, need a benchmark by a more exhaustive knowledge of nuclear fragmentation cross-sections. Several measurements were

made in the past, however most of them are limited to yields or total charge fragmentation cross-sections, in water or tissue equivalent (for a review see [6]), while the needed measurements of high precision  $d^2\sigma/d\theta dE$  double-differential cross-section (DDCS) are scarce [7]. Accurate knowledge of fragmentation cross sections would also be important in the field of space radiation risks assessment. The NASA space radiation program goal is to live and work safely in space with acceptable risks from radiation. With this aim, NASA promoted fragmentation cross sections studies [8], because of the ions present in the Galactic Cosmic Radiation (GCR) up to 400 MeV/nucleon. Moreover, GCR reach earth rarely, but become relevant for exposure into interplanetary flights, that are NASA future plans. Space radiation environment is made of different particles, among these only 1% are heavier ions, but although Iron ions ( $Z = 26$ ) are around 1/10 of C ( $Z = 6$ ) or O ( $Z = 8$ ) ions, their contribution to the absorbed equivalent dose is dominant.

In this picture, in the framework of an international collaboration, the FIRST (Fragmentation of Ions Relevant for Space and Therapy) experiment, at the SIS accelerator of GSI in Darmstadt, has been designed for measurements of ion fragmentation cross sections at different energies between 100 and 1000 MeV/nucleon.

## 2. The experimental set-up

Our set-up had to fulfill several requirements: from particle identification capability, providing a relative error  $\Delta M/M \leq 10\%$  for a clear separation of all ions and isotopes, tracking capability to measure angles and momenta of the produced charged fragments, large angular acceptance for the forward produced neutrons. A schematic layout of the FIRST experimental apparatus [9] is shown in Figure 1.

The detector consists of several sub-detectors divided in two main blocks: the Interaction Region (IR) and the Large Detector Region. The ALADIN magnet and the other detectors of the Large Detector Region have been inherited from previous experiments. Instead, all the detectors of the IR have been specifically designed and built for this experiment. These detectors have been tested with the Superconducting Cyclotron beams at INFN Laboratori Nazionali del Sud in Catania and at INFN Laboratori Nazionali di Frascati.

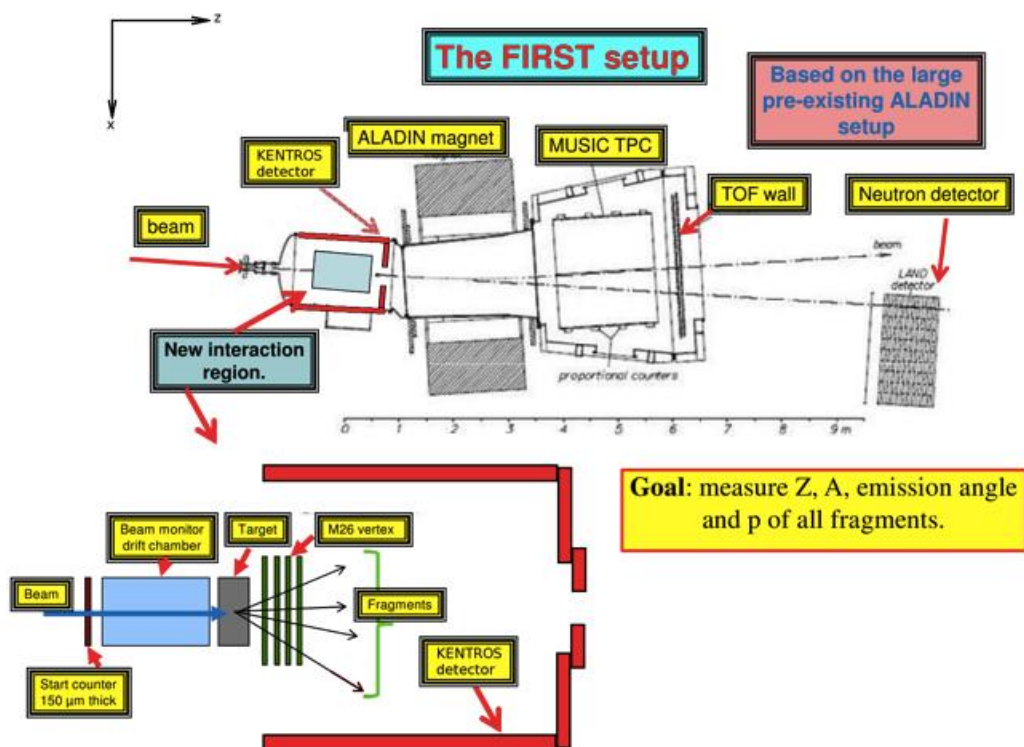


**Figure 1.** Schematic diagram of the FIRST experiment at GSI laboratory (up) and enlarged diagram of the interaction region (bottom).

Set-up redundancy allows systematic checks of the reconstructed particles features.

Following the beam path, the Start Counter [10] measures the starting time for time-of-flight measurement. The active part of this detector is a 52 mm diameter, 250 μm thick, EJ-228 fast scintillator foil. The scintillation signal is driven by four optical fiber bundles to four fast photomultipliers Hamamatsu H10721-201. The Start Counter efficiency was measured by using the unbiased sample of events triggered with the forward scintillator. It was found to be well above 99% in each of the runs, even when requiring the coincidence of all the 4 PMTs, thus providing an indication of the high quality of the light collection system. The time resolution was determined by means of a gaussian fit on the distribution of the time difference between pairs of PMTs. The sigma resulted all runs better than 150 ps. The time resolution is around 100 ps. The Beam Monitor [10] measures the incoming ion direction and the impact point on the target. It consists of a drift chamber filled by an Ar-CO<sub>2</sub> 80%-20% gas mixture and is composed by 36 sensing wires, arranged in 6 planes perpendicular to the beam, with the wires oriented alternatively in the horizontal and in the vertical direction. The space time relations used in the BM track reconstruction have been calibrated on a dedicated test beam [10] with a Carbon beam of 80 MeV/nucleon, performed at LNS in Catania, with same gas mixture at different HV. A track spatial resolution of 130-160 μm was achieved for all the C-C runs, in agreement with the expected performances for the BM detector. The Vertex Detector measures the tracks of charged particles originating from the target. It is based on the MIMOSA-26 silicon pixel sensor [11,12], which features an active area of

21.2x10.6 mm<sup>2</sup> segmented in 1152x576 pixels, with a 18.4  $\mu\text{m}$  pitch. The layout of the detector is shown in Figure 2.

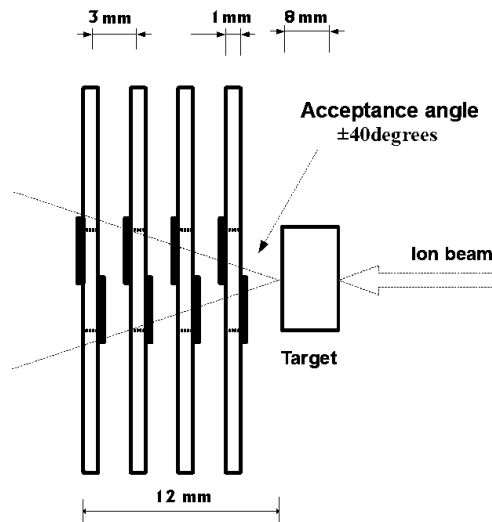


**Figure 2** Schematic horizontal layout of the Vertex Detector

It is composed by four planes of about 2x2 cm<sup>2</sup> area, each plane being made of two partially overlapping MIMOSA-26 detectors spaced by 3 mm and with the long side oriented vertically. It can measure tracks with an angular resolution of about 0.3 degrees up to polar angles of about 40 degrees. The KENTROS [13] (Kinetic ENergy and Time Resolution Optimized on Scintillator) detector measures the TOF and energy release of fragments with polar angles between about 5 degrees and 90 degrees, see Figure 3.

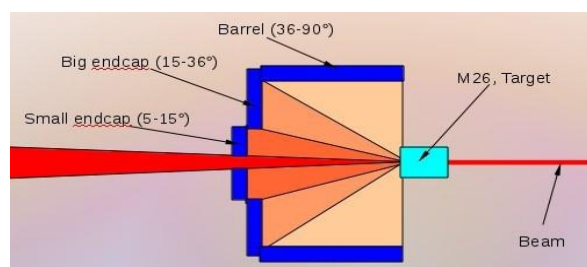


**Figure 3** Schematic layout of KENTROS detector

Those measurements are used to identify the particles and to evaluate their kinetic energy. The hits on the KENTROS detector can be matched to the tracks reconstructed by the vertex and beam monitor. For each detected particle, the information on the direction can be provided by the Vertex detector, while the particle type and kinetic energy can be obtained from the time of flight and energy deposition in the KENTROS modules. Those modules are made using EJ200 fast plastic scintillators. The scintillation signal is driven by plexiglass lightguides to AvanSiD Silicon Photo Multipliers (SiPM), 4x4 mm<sup>2</sup> active area.

The SiPM signal is read by custom readout boards, with individual supply voltage control, signal amplification, reshaping and splitting to charge ADCs and to TDCs. The cylindrical geometry of the KENTROS detector, with barrel and endcap subdetectors, was chosen in order to have the same symmetry as the physical process, so that the data analysis would not be complicated even if the modules have different efficiencies. The cylinder diameter was limited by space and cost considerations. The segmentation of the KENTROS detector was not related to the angular resolution, but it was rather a compromise between different needs:

- the efficiency in the collection of the scintillation signal increases with the ratio between the effective area of the SiPM and the cross-sectional area of the scintillator at the junction with the lightguide;
- the energy deposit increases with the detector thickness.

Since the SiPM effective area was fixed, the only way to increase the collection efficiency without reducing the thickness was to increase the number of modules as much as possible. For this reason, the barrel and the big endcap were segmented in 60 modules (however 10 modules from the barrel and 15 modules from the big endcap were missing in the first data acquisition). Furthermore, if a single endcap divided in 60 trapezoidal modules was used, the cross-sectional area of those elements at small angle would have been relatively very small and difficult to handle for high precision mechanical work and enveloping. For this reason, a small endcap with 24 modules was used for smaller polar angles. Those considerations led us to a final design with three subdetectors, i.e. the small endcap, the big endcap and the barrel, covering the polar angles between about 5 and 15 degrees, between about 15 and 36 degrees, and between about 36 and 90 degrees, respectively. The measured time resolution of the detector in our experimental conditions was of the order of 250 ps.

The large-detectors region include all detectors after the ALaDiN bending magnet. Following the beam path there is the MUSIC IV Time Projection Chamber, the TOF Wall and the LAND neutron detector. The TP-MUSIC IV (Time Projection Multiple Sampling Ionization Chamber) detector is a time projection chamber that measures the fragment tracks after the bending magnet. The active volume is filled by a P10 (10% Methane, 90% Argon) gas mixture, and it is divided in two equal parts by a cathode plane. The tracks projection on the yz plane is determined by proportional counters located on both sides of the detector, while the track projection on the bending (xz) plane is evaluated by measuring the ionization electrons drift time from the track to the proportional counters. The electronic readout is based on 14-bit FADCs, which digitize the signals coming directly from the preamplifiers. The MUSIC IV detector is able to measure with high efficiency and high resolution the charge and momentum of ions from He up to Au [14]. The TOF wall measures the arrival time, energy release and impinging position of the fragments produced with scattering polar angle smaller than about 6.5 degrees. It is composed by two layers, each made of 12 modules. Each module is composed by 8 BC-408 plastic scintillator slats, 110 cm long, 2.5 cm wide and 1 cm thick, oriented in the vertical direction. Each slat is read on both ends by two photomultipliers. The signal is split and read by Fastbus QDCs and by TDCs for charge and time measurements, respectively.

The Large Area Neutron Detector (LAND) [15] is a large scintillation detector, having an active volume of about  $2 \times 2 \times 1 \text{ m}^3$ , specifically designed for neutron detection. It is composed by 200 paddles having a volume of  $200 \times 10 \times 10 \text{ cm}^3$ . Each paddle is made of 11 sheets of iron alternated with 10 sheets of scintillator. The scintillation light is collected on both ends of the paddles by stripe light guides, which drive it to the photomultipliers. The difference in the arrival times of the two signals is used to localize the position where the neutron interacts with the scintillator material, while the mean time is used to evaluate the neutron TOF.

### 3. The FIRST data taking at GSI

The FIRST experiment was mounted at the GSI laboratory and a first data taking was carried out between July and August 2011. Most of the measurements were made using a 400 MeV/nucleon  $^{12}\text{C}$  beam on 8 mm thick carbon target. Some runs were made using a 0.5 mm thick gold target, while the remaining measurements were made for testing and/or calibration purpose. The data acquisition (DAQ) was managed through the Multi Branch System (MBS) DAQ framework developed at GSI [16]. This system can handle all the front end electronics standards (FASTBUS, CAMAC and VME) used in the experiment. Each readout crate was equipped by a trigger module, and all those modules were connected through a trigger bus to distribute the trigger and dead-time signals and to ensure events synchronization. A logical combination of the trigger signals from different detectors was used to produce the global trigger decision. Basically, this decision was based on the coincidence of the Start Counter trigger with any of the TOF Wall, LAND or KENTROS trigger. Furthermore, in order to suppress the events in which the carbon ion did not interact with the target, coincidences between the SC and a Veto Counter were rejected.

The event acquisition rate was limited by the dead time, which was determined by the conversion time in the digitization modules and transfer data time from the electronics to the readout controllers and from the controllers to the event builder. Unfortunately, during the experiment it was not possible to use the MUSIC IV detector due to an anomalous increase of the current in the main cathode, whose origin must be still investigated.

A total number of about 37 million events were acquired in this data taking. The data analysis is in progress. From the preliminary analysis, the measured values of the detector resolutions and the quality of the data seem to be in agreement with the goals of the project. An example of distribution from the data acquired in this data taking is shown in Figure 4, which represents the scatter plot of the TDC counts as a function of the ADC counts measured by a single slat of the TOF Wall for the 400 MeV/nucleon C-C runs, without calibration.

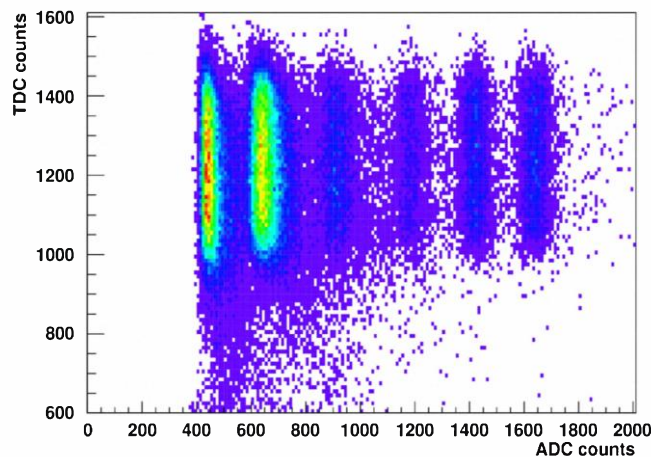


**Figure 4** TDC vs ADC counts on TOF Wall on a single slat.  
The regions in the plot correspond to the ion fragments  $Z=1, \dots, 6$ .

Through the global track reconstruction, the time-of-flight information will be used to evaluate the fragments kinetic energies.

Another example of distribution obtained in the preliminary analysis of the data is shown in Figure 5, which represents the TDC time as a function of the QADC counts measured by a single module of the KENTROS Small Endcap, which cover the scattering polar angles between 5 and 15 degrees.



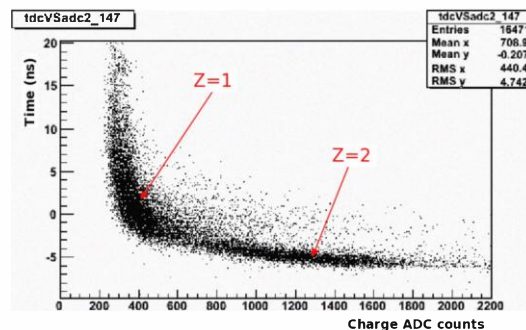


**Figure 5** TDC time versus QADC counts on a Small Endcap module of the KENTROS detector, for the 400 MeV/u C-C runs, with no calibration and no time-walk correction. The two regions in the scatter plot correspond to fragments  $Z=1$  and  $Z=2$ .

The shape of the distribution is influenced by the time-walk effect, which must be corrected. The two regions in the scatter plot on the top-left and on the bottom right correspond to the ion fragments with  $Z=1$  and  $Z=2$ , respectively. The time of flight and the energy release, combined with the information on the tracks reconstructed by the vertex detector, will be used to evaluate the fragment kinetic energy.

#### 4. Conclusions

The FIRST experiment was designed for the measurements of nuclear fragmentation DDCS, with respect to kinetic energy and scattering polar angle, for light ions in the range between 100 and 1000 MeV/nucleon. The experiment was mounted at the GSI laboratory, and there was a first data taking during August 2011. About 37 million events were acquired in this data taking, mainly using a 400 MeV/nucleon  $^{12}\text{C}$  beam on a carbon target. The data analysis is still in progress. However, from the preliminary analysis, the measured values of the detector resolutions and the quality of the data seem to be in agreement with the goals of the project.

#### 5. References

- [1] G.Kraft 2000 "Tumor therapy with heavy charged particles", *Progress in particle and Nuclear Physics* **45** 473-544
- [2] E. Haettner, H. Iwase, D. Schardt 2006 "Experimental fragmentation studies with  $^{12}\text{C}$  therapy beams", *Radiation Protection Dosimetry* **122** 485-487
- [3] M. Kramer and M. Durante 2010 "Ion beam transport calculations and treatment plans in particle therapy", *European Physical Journal D* **60** 195-202
- [4] L.Sihver and D.Mancusi 2009 "Present status and validation of HIBRAC", *Radiation Measurements* **44** 38-46
- [5] T.Bohlen et al. "Benchmarking nuclear models of FLUKA and GEANT4 for carbon ion therapy" 2010 *Physics in Medicine and Biology* **55** 5833-5847
- [6] D.Schardt, T.Elsasser, D.Schulz-Ertner 2010 "Heavy-ion tumor therapy: Physical and radiobiological benefits", *Reviews of Modern Physics* **82** 383-425
- [7] C. Agodi et al., 2007 "Heavy ions fragmentations measurements at intermediate energies in hadrontherapy and spatial vehicles shielding", *IEEE NSS* **1** 790-792
- [8] J.W. Norbury and J. Miller 2011 *47th NCRP Annual Meeting*, Bethesda, MD, 24
- [9] R.Pleskac et al. 2012 "The FIRST experiment at GSI", *Nuclear Instrument and Methods in Physics Research A* **678** 130-138

- [10] Z.Abou-Haidar et al. 2012 “Performance of upstream interaction region detectors for the FIRST experiment at GSI”, *Journal of Instrumentation* **7**
- [11] <http://www.iphc.cnrs.fr/-CMOS-ILC-.html>
- [12] E. Spiriti et al., 2011, "The FIRST experiment: Interaction region and MAPS vertex detector", *Nuclear Physics B - Proceedings Supplements*, **215**: 157-161.
- [13] B. Golosio et al., "The FIRST experiment for nuclear fragmentation measurements at GSI", *IEEE Nuclear Science Symposium Conference Record*. 2277-2280, 2012.
- [14] C. Sfienti et al. 2009 "Isotopic dependence of the nuclear caloric curve" *Physical Review Letters* **102** 15
- [15] P. Pawlowski et al.,” Neutron recognition in the LAND detector for large neutron multiplicity”, *Nuclear Instrument and Methods in Physics Research A* **694** 47-54
- [16] H.G.Essel and N.Kurz 2000 "The general purpose data acquisition system MBS" *IEEE TNS* **47** 337-339